



Rapid and label-free cell detection by metal-cluster-decorated carbon nanotube biosensors

Fumiaki N. Ishikawa^a, Beth Stauffer^b, David A. Caron^b, Chongwu Zhou^{a,*}

^a Department of Electrical Engineering, University of Southern California, 3710 McClintock Ave, Los Angeles, CA 90089, United States

^b Department of Biological Sciences, University of Southern California, Los Angeles, CA 90089, United States

ARTICLE INFO

Article history:

Received 19 December 2008

Received in revised form 15 February 2009

Accepted 2 March 2009

Available online 14 March 2009

Keywords:

Biosensor

Carbon nanotube

Aureococcus anophagefferens

Environmental monitoring

ABSTRACT

In this paper, the use of carbon nanotube biosensors toward alga cell detection was examined. The biosensor devices were fabricated on complete 4 in. wafers by first growing carbon nanotubes (CNTs) and then depositing metal electrodes using a shadow mask. In addition, we decorated the biosensors with metal-clusters resulted in enhancing the sensitivity by 2000-folds and has enabled the detection of streptavidin down to 10 pM concentration. This sensitivity enhancement was attributed to activation of CNT channels due to formation of Schottky junctions between CNTs and metal-clusters. Real-time cell detection has been successfully carried out using the CNT biosensors for two kinds of alga related to brown tides: *Aureococcus anophagefferens* and BT3. Functionalization of the CNT biosensors with the monoclonal antibody for *A. anophagefferens* has led to detection at a concentration of 10⁴ cells/ml, with sensitivity lower than 10⁴ cells/ml projected based on the signal-to-noise ratio of the sensors. Further functionalization with tween 20 led to suppression of non-specific binding of BT3 and enabled label-free and selective detection of *A. anophagefferens*. These nanobiosensors may find potential applications for environmental monitoring and disease diagnosis.

© 2009 Elsevier B.V. All rights reserved.

1. Introduction

Detection of chemical agents and biological species using nanostructured materials has shown significant progress in recent years, driven by the high demand for superior analytical tools in areas such as environmental monitoring, new drug screening, and disease diagnostics. Various detection techniques have been proposed and demonstrated using a wide variety of nanomaterials (Elghanian et al., 1997; Gerion et al., 2003; Kong et al., 2000; Star et al., 2006a; Hu et al., 2007; Kind et al., 2002; Kolmakov et al., 2005; Grossman et al., 2000). Among such emerging technologies, detection of biomolecules using semiconducting nanowire (NW) and carbon nanotube (CNT) field effect transistors (FETs) has attracted considerable interest, since it offers excellent sensitivity owing to large surface-to-volume ratios of NWs and CNTs, label-free detection, real-time sensing, and apparatus simplicity (electrical read out). The successful detection of various biological species with excellent performance using such NW/CNT devices testifies to the great potential of this novel technology (Cui et al., 2001; Chen et al., 2003; Star et al., 2003, 2006b; Li et al., 2004, 2005; Bunimovich et al., 2006; Stern et al., 2007; He et al., 2007; Byon and Choi, 2006; So et al., 2005; Gui et al., 2007).

In spite of these successful demonstrations, application of such nanobiosensors toward cell identification remains relatively unexplored (Panchapakesan et al., 2005; Shao et al., 2008). Accurate, sensitive and rapid identification of cells is, however, extremely important in areas such as medical diagnosis, biological research, and environmental monitoring. As an example, *Aureococcus anophagefferens* (*A. anophagefferens*) is a noxious, 2–3 μm pelagophyte alga that has been shown to cause outbreaks of 'brown tides' in estuaries of the mid-Atlantic coastal of the U.S. (Anderson et al., 1989). High abundances of this alga have devastating environmental impact and adversely effect commercial shellfisheries. *A. anophagefferens* has few distinguishing morphological features, and therefore cannot be differentiated from non-toxic, co-occurring species such as BT3. Considerable effort has been made toward the development of detection tools for *A. anophagefferens* (Popels et al., 2003; Aridgides et al., 2004).

Conventionally, immunofluorescent staining of *A. anophagefferens* with a polyclonal antibody followed by a manual counting using a microscope has been widely employed to enumerate *A. anophagefferens* (Aridgides et al., 2004). Recently, a colorimetric, enzyme-linked immunosorbent assay (ELISA) performed in 96-well microtiter plates was developed for more rapid quantification of *A. anophagefferens* in large numbers of samples (Caron et al., 2003). However, those techniques require multiple steps for labeling, which limits the throughput, and also a bulky and expensive optical setup is needed for the measurement. In addition, those techniques

* Corresponding author.

E-mail address: chongwuz@usc.edu (C. Zhou).

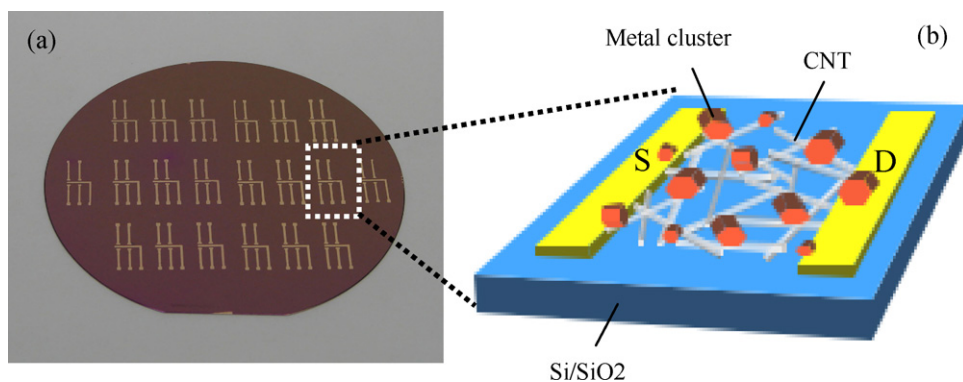


Fig. 1. (a) An optical micrograph of devices on a complete 4 in. wafer. (b) Schematic diagram of the device.

largely depend on manual operations which require intensive training on the user. For further facilitation of biological research on brown tide, it is desirable to improve and/or develop new technologies with features such as cost-effective, on-site, real-time, and label-free sensing capability with minimal human intervention.

In this context, we demonstrate real-time and label-free detection of *A. anophagefferens* using metal-cluster-decorated carbon nanotube biosensors. Our CNT based electrical biosensors have advantages that complement the previously developed methods and are ideal for on-site and portable detection system, such as compact setup without bulky equipments, direct electrical read-out, automated data acquisition with minimal human intervention, high throughput, and easy operation. The devices were fabricated by growing carbon nanotubes on complete 4 in. wafers and depositing metal electrodes, which demonstrates highly manufacturable production of the sensors. Furthermore, the biosensor sensitivity was improved by 2000-folds using a highly controllable and reproducible metal-cluster-decoration technique. This led to the detection of streptavidin, which was used as a model case, at a concentration of 10 pM. Real-time cell detection has been successfully carried out using the CNT biosensors for both *A. anophagefferens* and *BT3*, with sensitivity down to 10^5 and 10^4 cells/ml, respectively. Monoclonal antibody for *A. anophagefferens* was used to functionalize the device, and it led to detection of *A. anophagefferens* at a concentration of 10^4 cells/ml with a signal-to-noise ratio of ~ 7 , which suggests possible sensitivity lower than 10^4 cells/ml. Further functionalization with tween 20 led to suppression of non-specific binding of *BT3* and enabled label-free and selective detection of *A. anophagefferens*. These nanobiosensors have great potential for environmental monitoring and disease diagnosis.

2. Materials and methods

2.1. Device fabrication

CNTs were grown on a degenerately doped Si wafer with 500 nm SiO₂ on top via chemical vapor deposition (CVD) method with Fe nanoparticles formed from ferritin molecules as catalysts. Diluted solution of ferritin in de-ionized water (D.I. water) was put on the Si/SiO₂ wafer and kept for 1 h at room temperature, resulting in deposition of ferritin molecules onto the substrate. The substrate was then washed with D.I. water, followed by calcination in air at 700 °C for 10 min, allowing formation of Fe nanoparticles. After the calcination, the substrate placed in a quartz tube was heated to 900 °C in hydrogen atmosphere, and once the temperature reached 900 °C, methane (1300 sccm), ethylene (20 sccm), and hydrogen (600 sccm) were flowed into the quartz tube for 10 min, which yields a CNT network on the substrate. Following the growth was patterning of source-drain electrodes, done by depositing 10 nm Cr

and 30 nm Au through a Cu shadow mask. The channel width and length of the resultant devices were 5 mm and 100–200 μm, respectively. Oxygen plasma was then performed for 1 min in order to etch unwanted CNTs while covering the channel areas with poly(methyl methacrylate) (PMMA). Metal-clusters were then deposited onto entire devices to improve sensitivity as shown later, which was done by evaporating 3 Å Cr and 5 Å Au using an e-beam evaporator. Fig. 1a shows an optimal micrograph of the biosensor array on a complete 4 in. wafer after whole process, with a schematic diagram of the device structure shown in Fig. 1(b). A device yield of 100% was easily accomplished through our fabrication, due to the use of nanotube networks (Snow et al., 2006). The device uniformity was statistically analyzed, and a histogram of the device resistances produced through one round of fabrication is shown in Fig. S1. A gaussian fit to the histogram (the blue line in Fig. S1) reveals a mean of 31.20 kΩ and a standard deviation of 8.32 kΩ. 56% of the devices exhibited resistance in a narrow range of 20–60 kΩ.

2.2. Electrical measurement

For biosensing in solution, the device was firstly mounted onto a homemade teflon cell, and 0.2 ml of phosphate buffered saline (PBS) (pH 7.4, 0.14 M NaCl) was injected into the cell. A Pt wire was inserted into the buffer, which acts as a reference electrode (ground potential) during sensing. The schematic diagram is shown in Fig. S2. Drain–source voltage (V_{ds}) of 10 mV was then applied while keeping the Pt wire at ground potential, and I_{ds} was monitored during solutions of interest (10–20 μl) were added to the buffer. We note that at least three devices were tested for each measurement, and all devices showed similar behavior. We also note that the figures shown are the typical results for each experiment. The concentrations of proteins and cells shown in following tests and figures represent the actual concentrations to which the devices were exposed. We emphasize that the whole measurement setup is compact that fits within 30 cm × 50 cm area as shown in Fig. S3.

2.3. Cell preparation

Cells used in this study were prepared following Ref. 25. Strain CCMP1794 of *A. A.* from Barnegat Bay, New Jersey, was cultured in modified f/2 medium at 20 °C under a 12:12 h light:dark cycle in an incubator with light intensity of $\sim 200 \mu\text{E m}^{-2} \text{s}^{-1}$. A culture of *BT3* (unidentified coccoid cell), which was isolated from a brown tide in Great South Bay, NY in November of 1986, was grown in f/2 medium (minus silica) at 20 °C. Cells were harvested in late exponential phase and preserved with a final concentration of 1% glutaraldehyde. Cells were filtered onto 0.22 μm Millipore filters and subsequently resuspended in 10 mM PBS-T (Sigma). Cell

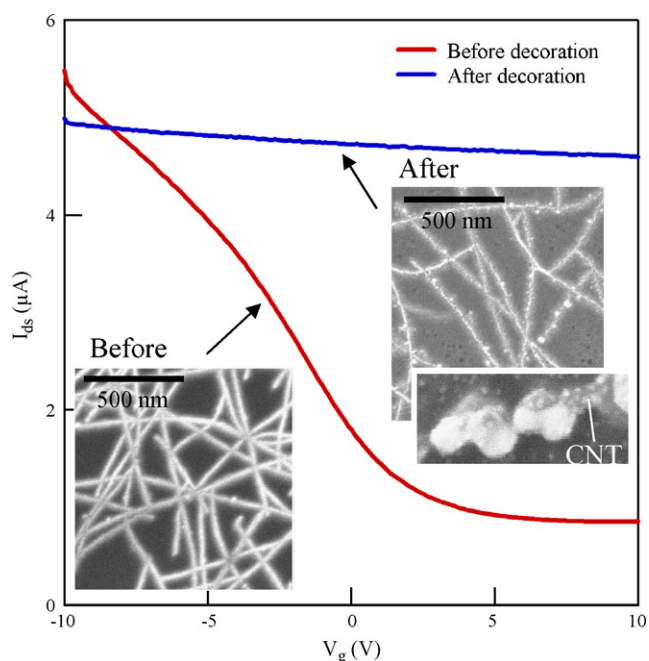


Fig. 2. Source-drain current (I_{ds}) versus gate voltage (V_g) before (red) and after (blue) the cluster deposition. Insets: SEM images of carbon nanotubes before and after the cluster deposition, respectively. (For interpretation of the references to color in this figure legend, the reader is referred to the web version of the article.)

abundances were determined using a hemacytometer and standard microscopical counting techniques.

3. Results and discussion

Interestingly, we found that by adapting a simple metal deposition technique, one can obtain significant sensitivity improvement for the CNT biosensors decorated with metal-clusters. Deposition of metal-clusters onto CNTs/NWs was reported to efficiently enhance the sensitivity of chemical sensing devices (Kolmakov et al., 2005; Star et al., 2006a; Kong et al., 2001), but the effect of metal-cluster-decoration on biosensing has not been investigated or reported. In this study, we demonstrate using metal-cluster deposition to improve the performance of biosensors for the first time. Though increased sensitivity was previously demonstrated by angle deposition of metal contacts using a shadow mask for carbon nanotube network biosensors (Byon and Choi, 2006), this process can be hard to control. Compared to this method, our technique reported here has better controllability and easy to reproduce. The SEM images of the CNTs before and after the deposition are shown in the insets of Fig. 2, which clearly show the formation of metal-clusters on the CNTs. Fig. 2 shows the source–drain current (I_{ds}) versus gate voltage (V_g) measurements in air on the devices before/after the cluster deposition. An increased conductance by a factor of 2.63 at $V_g = 0$ V and disappearance of gate dependence were observed after the cluster deposition. The weakened gate dependence is believed to be due to screening effect by the metal-clusters. Screening effect is shielding of an electric field by materials, which is a well-known phenomenon. (Israelachvili, 1991). When there are metal-clusters on nanotubes, the electric field induced by the gate potential is screened by the metal-clusters, and thus the gate dependence of the nanotube device is weakened. A similar trend has been reported previously, where sensitivity enhancement was also demonstrated by angle deposition of metal contacts (Byon and Choi, 2006).

Sensitivities of the devices with or without the metal-cluster coating were subsequently compared using streptavidin (SA) as a model case. The sensing responses of device conductance (G) nor-

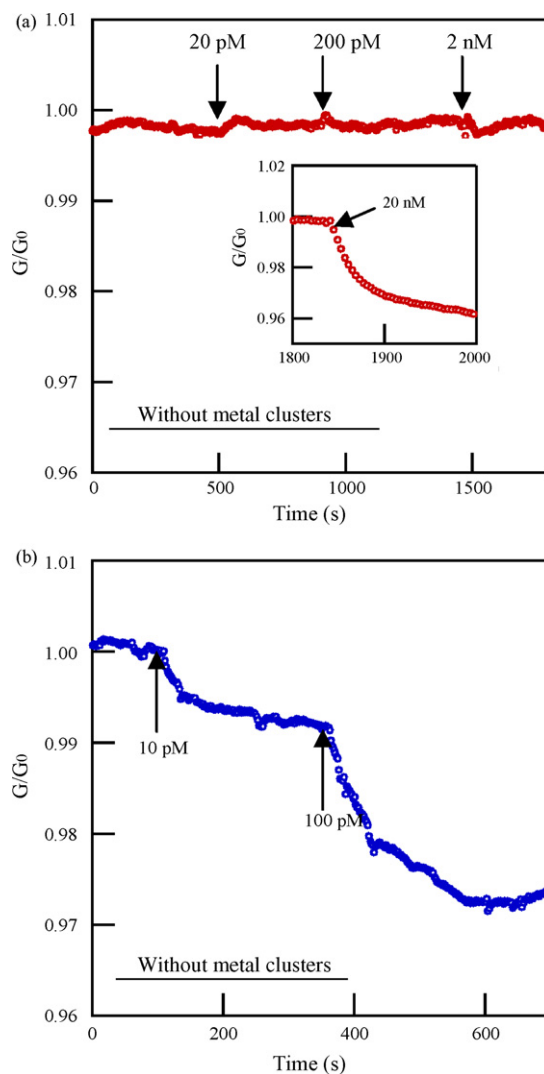


Fig. 3. Plots of normalized conductance versus time during exposure to streptavidin solutions with different concentrations for devices without metal-cluster coating, and with metal-cluster coating, respectively. The inset in (b) shows detection of streptavidin of 20 nM.

malized by initial conductance (G_0) plotted versus time for devices without and with metal-clusters are shown in Fig. 3(a) and (b), respectively. The arrows in the figures indicate the timing when SA solutions of each concentration were exposed to the devices. As shown in Fig. 3(a), the device without metal-clusters exhibited no conductance change upon exposure to SA solutions up to 2 nM, and a conductance drop by $\sim 4\%$ was observed only after exposure to a SA solution of 20 nM (Fig. 3(a) inset). The device with metal-clusters, on the other hand, exhibited pronounced sensitivity, as shown in Fig. 3(b), where a conductance drop of $\sim 1\%$ appeared upon exposure to SA of 10 pM, and another drop of $\sim 3\%$ was observed upon exposure to 100 pM SA. Several devices with/without metal-clusters were tested, and consistent results were observed. That is, devices with metal-clusters exhibited higher sensitivity than devices without metal-clusters by two to four orders of magnitude. More information can be found in Fig. S4, which shows the measured data from two other devices.

We attribute the mechanism of the sensitivity improvement to activation of carbon nanotubes by formation of Schottky junctions between the deposited metal-clusters and CNTs. Previous report by Chen et al. (2004) has suggested that transport properties of CNT devices are more susceptible to protein adsorptions at the vicin-

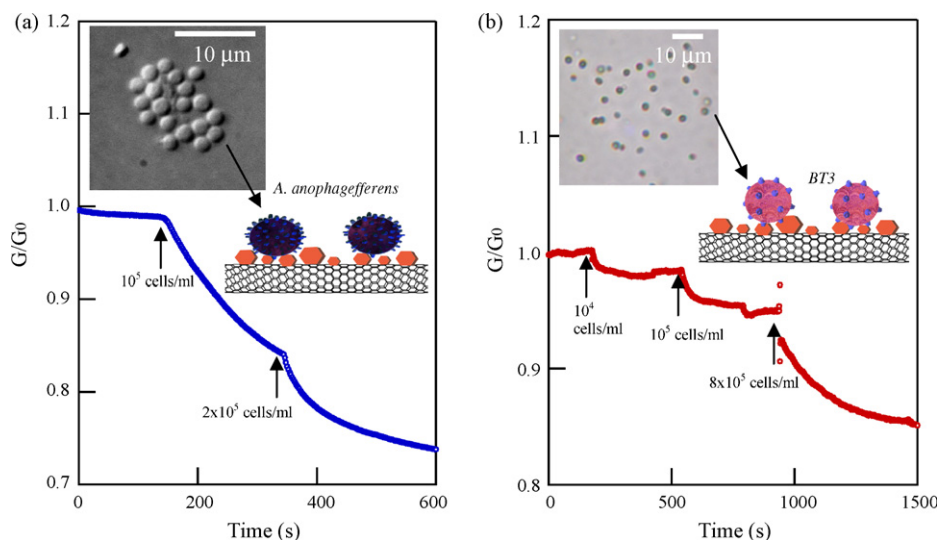


Fig. 4. Plots of normalized conductance versus time during exposure to *A. anophagefferens* and *BT3*, respectively. The insets at the top are optical images of *Aureococcus anophagefferens* (*A. anophagefferens*) and *BT3* cells, respectively. The insets at the middle are schematic illustrations of *A. anophagefferens* and *BT3* on the devices with metal-clusters, respectively.

ity of metal–CNT interfaces rather than at CNT channels. Similar observations were also made for DNA sensing using CNT biosensors (Gui et al., 2007; Tang et al., 2006). Based on our observation and these reports, we suggest that deposition of metal-clusters onto CNTs increases the number of metal–CNT junctions, which results in increased number of “hotspots”, where adsorption of proteins can modulate the transport properties around the spots most efficiently. This scenario is schematically illustrated in Fig. S5. Further control experiments were also performed, where we used nanotube sensors with the source and drain contacts passivated by PMMA. The detail can be found in Fig. S6. Briefly speaking, the passivated devices without metal-cluster-decoration exhibited no response to 100 nM SA. This is consistent with previous report and can be understood as the metal electrode/nanotube Schottky junction is shielded from SA adsorption. In contrast, similar devices with metal-cluster-decoration displayed significant conductance drop after exposure to 100 nM SA. This confirms the important role of the metal-cluster/nanotube Schottky junctions. We estimated the density of metal-clusters to be 2–3/100 nm² from the SEM image in Fig. 2. This density could be controlled by evaporating the metal of different thickness. We expect that increasing the density of metal-clusters would result in more number of hot spots, thus increase the sensitivity. However, when the density of metal-clusters reaches a point where they start to form a continuous pathway, it will form metallic wires coating nanotubes that would not respond to biomolecules. As a result, it is expected that maximum sensitivity will be achieved when the density of metal-cluster is optimized.

With the devices described here, a series of systematic studies were conducted, which led to the demonstration of selective algal sensing. First, non-specific binding of algal cells on the devices was investigated. Devices with the metal decoration were exposed to suspensions of two types of cells, *A. anophagefferens* and *BT3*, and electrical conduction through the devices was monitored during the exposure. *BT3* is a co-occurring microalga (it is similar in size and morphology to *A. anophagefferens* but is a different golden alga with no known toxic effects), and was used as a control sample to demonstrate specificity to *A. anophagefferens*. Light micrographs of *A. anophagefferens* and *BT3* are displayed in the insets of Fig. 4(a) and (b), respectively, indicating their similar morphologies. Non-specific binding of both cells, as illustrated in schematic diagrams shown as insets in Fig. 4(a) and (b), respectively, had significant influences on the device conductance. The normalized conductance

plotted versus time is shown in Fig. 4(a), where the exposure to a suspension of *A. anophagefferens* of 10⁵ cells/ml induced a conductance decrease of ~26%, and further exposure to a suspension of 2 × 10⁵ cells/ml resulted in additional conductance decrease of ~12%. Non-specific binding of *BT3* was also found to decrease the device conductance by 2% with concentrations of 10⁴ cells/ml, an additional 3% with 2 × 10⁴ cells/ml, and an additional 10% with 10⁵ cells/ml, respectively (Fig. 4(b)). We temporarily attribute the decrease in conductance to the modulation of the metal/nanotube Schottky junction by the biological moieties on the cell membranes such as receptor proteins. This will be discussed later again. Nevertheless, this experiment reveals that CNT biosensors (with metal coating) are able to sense the binding of algal cells, while care must be taken to suppress non-specific binding to establish selectivity as in the case for protein and DNA sensing (Chen et al., 2003; Star et al., 2006b; Byon and Choi, 2006; So et al., 2005).

Coating with a surfactant, tween 20, which has been used to prevent non-specific binding of proteins onto many solid surfaces including CNTs (Chen et al., 2003; Byon and Choi, 2006; So et al., 2005; Williams et al., 2006; Lee et al., 2002; Agudelo and Portus, 2000) was adopted here toward suppression of algal cell non-specific binding. One control experiment was performed to examine the feasibility of this strategy, and the result suggested that coating with tween 20 was able to suppress the non-specific binding of algal cells. The details can be found in the supporting information (Fig. S7).

For selective detection of algal cells, devices must be functionalized with a receptor to selectively capture the target alga. Here we adopted the previously developed monoclonal antibody (MAb) for *A. anophagefferens* as the receptor molecule (Caron et al., 2003). A control experiment was first conducted to examine our chemistry for immobilization of the MAb and sensing capability of the devices upon the functionalization. Non-specific binding due to hydrophobic interaction was used to attach the MAb of *A. anophagefferens* to metal-cluster-decorated devices as follows. The nanotube biosensor chip was first washed with acetone and isopropanol for 15 min each, and 40 μl of the MAb solution was introduced to cover the device. The chip was immediately placed in a fume hood and kept at 0–4 °C for 24 h. The presence of metal-clusters made the use of AFM inappropriate to examine immobilization of the MAb, but immobilization of the MAb was confirmed by the decreased conductance of the device after the binding of MAb (data not shown).

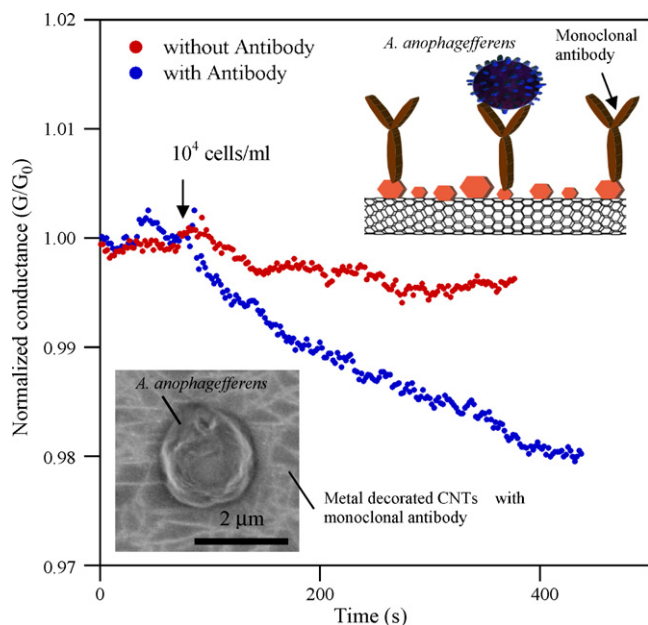


Fig. 5. Normalized conductance versus time plot of a device with (blue)/without (red) monoclonal antibody during exposure to solutions of *A. anophagefferens*. The inset at the top is a schematic of a device with antibody capturing *A. anophagefferens* cells. The inset at the bottom is a SEM image of alga cell captured onto CNT network decorated with metal-clusters and antibody. (For interpretation of the references to color in this figure legend, the reader is referred to the web version of the article.)

The sensing capability of the device was subsequently examined. The device structure following functionalization is illustrated as an inset of Fig. 5. The conductance versus time plot is shown in Fig. 5. For comparison, the plot for a device without MAb is also shown. The device with MAb responded to a suspension of 10^4 cells/ml of *A. anophagefferens* with a decreased conductance of $\sim 2\%$, while the device without MAb showed only $\sim 0.5\%$ change to a suspension of *A. anophagefferens* at same concentration. The enhanced response could be due to the increased binding capacity of the device toward *A. anophagefferens* by the aid of MAb. The capturing of *A. anophagefferens* was directly confirmed by visual inspection of the devices with SEM after the sensing experiments. We observed

several of captured *A. anophagefferens* cells on CNT network decorated with metal-clusters and with MAb, as shown in the inset of Fig. 5 of the SEM image (only one cell is present in this figure). We note that modulation of Schottky junctions by capturing DNAs/proteins by probe molecules covering the nanotube-metal Schottky junctions has been reported in several reports (Chen et al., 2004; Gui et al., 2007; Tang et al., 2006). The antibody used in our study is similar in size to these antibodies, and therefore the binding of *A. anophagefferens* on the antibody is believed to modulate the Schottky junctions and result in the conductance change. This experiment confirms the successful functionalization of our biosensor with MAb. Furthermore, our data clearly shows significant sensing signal amplitude for 10^4 cells/ml, and thus the lowest detection limit for the sensors could be smaller than 10^4 cells/ml.

Finally, selective sensing of *A. anophagefferens* was demonstrated by coupling the above developed chemistry. The functionalization of devices for this experiment was done by first immobilizing the MAb in the same manner as the above-mentioned experiment. The devices were subsequently soaked in a tween 20 solution for passivation of the remaining exposed nanotubes, metal-clusters, and metal contacts. Following functionalization, selectivity of the device was tested as shown in the schematic diagram of our sequential operation for selective sensing (Fig. 6(a)). The corresponding conductance versus time plot is shown in Fig. 6(b). First, the device was exposed to a suspension of BT3 (8×10^5 cells/ml) at $t = 46$ s (step II in Fig. 6(a)), and this caused negligible conductance change within 100 s. A suspension of *A. anophagefferens* was then introduced into the buffer (step III in Fig. 6(a)), and a conductance drop by $\sim 2\%$ was observed, indicating selective capture of *A. anophagefferens*. This experiment clearly demonstrates that our sensor is capable of sensing *A. anophagefferens* selectively over BT3.

4. Conclusions

In summary, our study has revealed that CNT biosensors have great potential to achieve highly cost-effective detection of harmful *A. anophagefferens* with on-site, rapid and label-free sensing capability. Such sensors were made through a highly manufacturable method, and the sensitivity was improved by a factor of 2000 using metal-cluster coating, with streptavidin as an example. The metal-cluster-decoration should be a generic effect, and we

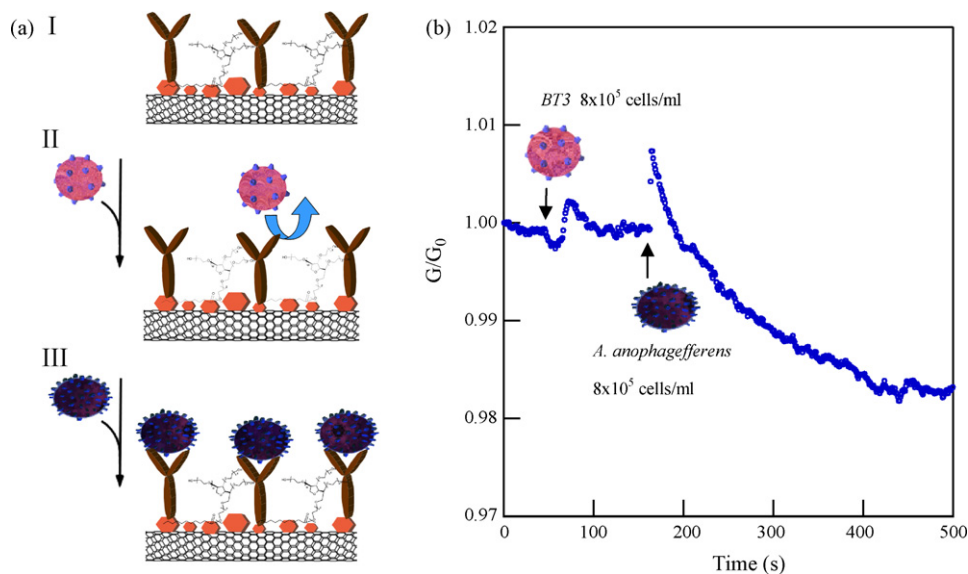


Fig. 6. (a) Schematic illustration of the sequential operations to demonstrate selective recognition of *A. anophagefferens* cells. (b) Normalized conductance versus time plot during sequential exposure to BT3 and *A. anophagefferens*, for a device with antibody and tween 20 functionalization.

believe other metals that can form Schottky junctions with nanotubes can deliver similar performance. Non-specific binding of *A. anophagefferens* and *BT3* was found to cause conductance drops in metal-cluster-decorated CNT biosensors. The devices were functionalized with monoclonal antibody for *A. anophagefferens*, and used to detect *A. anophagefferens* at a concentration of 10^4 cells/ml, with possible sensitivity lower than 10^4 cells/ml judged from the signal-to-noise ratio. Tween 20 coating was used to suppress signaling due to non-specific binding of *BT3*. Finally, combined with an immunological approach, our device exhibited selective detection of *A. anophagefferens* against another microalga (*BT3*). Comparing our approach with previous methods, our approach has proved the advantages such as rapid analysis (~10 min), compact and inexpensive detection system, and easy operation as expected, while maintaining moderate sensitivity (possible lowest detection limit $<10^4$ cells/ml) and detection range up to 10^6 cells/ml. The sensitivity may be further improved by fine-tuning/innovating the device fabrication and functionalization, such as catalyst size/material, nanotube density, growth condition, channel length, contact material, metal-cluster-decoration, and use of a linker molecule to attach monoclonal antibody. Overall, while there is still room for improvement, our study has successfully proved the concept of using CNT biosensors as an inexpensive, convenient, and user-friendly detection scheme for *A. anophagefferens*. Furthermore, our approach of electrical, rapid, inexpensive, and label-free detection of algal cells can be easily expanded toward detection of other types of cells, such as pathogenic bacterial cells for food monitoring, and malignant cells for diagnosis.

Acknowledgement

We gratefully acknowledge support from Whittier Foundation and National Institutes of Health, and National Science Foundation Grants CCR-0120778 (Center for Embedded Networked Sensing; CENS).

Appendix A. Supplementary data

Supplementary data associated with this article can be found, in the online version, at doi:10.1016/j.bios.2009.03.001.

References

- Agudelo, S., Portus, H., 2000. *Clinical and Diagnostic Laboratory Immunology* 7, 717–718.
- Anderson, D.M., Kulis, D.M., Cosper, E.M., 1989. *Novel phytoplankton blooms: causes and impacts of recurrent brown tides and other unusual blooms*. Springer-Verlag, Berlin.

- Aridgides, L.J., Doblin, M.A., Berke, T., Dobbs, F.C., Matson, D.O., Drake, L.A., 2004. *Marine Pollution Bulletin* 48, 1096–1101.
- Bunimovich, Y.L., Shin, Y.S., Yeo, W.S., Amori, M., Kwong, G., Heath, J.R., 2006. *Journal of the American Chemical Society* 128, 16323–16331.
- Byon, H.R., Choi, H.C., 2006. *Journal of the American Chemical Society* 128, 2188–2189.
- Caron, D.A., Dennett, M.R., Moran, D.M., Schaffner, R.A., Lonsdale, D.J., Gobler, C.J., Nuzzi, R., Mclean, T.L., 2003. *Applied and Environmental Microbiology* 69, 5492–5502.
- Chen, R.J., Bangsaruntip, S., Drouvalakis, K.A., Kam, N.W.S., Shim, M., Li, Y.M., Kim, W., Utz, P.J., Dai, H.J., 2003. *Proceedings of the National Academy of Sciences of the United States of America* 100, 4984–4989.
- Chen, R.J., Choi, H.C., Bangsaruntip, S., Yenilmez, E., Tang, X.W., Wang, Q., Chang, Y.L., Dai, H.J., 2004. *Journal of the American Chemical Society* 126, 1563–1568.
- Cui, Y., Wei, Q.Q., Park, H.K., Lieber, C.M., 2001. *Science* 293, 1289–1292.
- Elghanian, R., Storhoff, J.J., Mucic, R.C., Letsinger, R.L., Mirkin, C.A., 1997. *Science* 277, 1078–1081.
- Gerion, D., Chen, F.Q., Kannan, B., Fu, A.H., Parak, W.J., Chen, D.J., Majumdar, A., Alivisatos, A.P., 2003. *Analytical Chemistry* 75, 4766–4772.
- Grossman, H.L., Chemla, Y.R., Lee, T.S., Clarke, J., Adamkiewicz, M., Buchanan, B.B., 2000. *Biophysical Journal* 78, 267A–1267A.
- Gui, E.L., Li, L.J., Zhang, K.K., Xu, Y.P., Dong, X.C., Ho, X.N., Lee, P.S., Kasim, J., Shen, Z.X., Rogers, J.A., Mhaisalkar, S.G., 2007. *Journal of the American Chemical Society* 129, 14427–14432.
- He, J.H., Zhang, Y.Y., Liu, J., Moore, D., Bao, G., Wang, Z.L., 2007. *Journal of Physical Chemistry C* 111, 12152–12156.
- Hu, C.G., Feng, B., Xi, Y., Zhang, Z.W., Wang, N., 2007. *Diamond and Related Materials* 16, 1988–1991.
- Israelachvili, J.N., 1991. *Intermolecular & Surface Forces*, 2nd ed. Academic Press, London.
- Kind, H., Yan, H.Q., Messer, B., Law, M., Yang, P.D., 2002. *Advanced Materials* 14, 158.
- Kolmakov, A., Klenov, D.O., Lilach, Y., Stemmer, S., Moskovits, M., 2005. *Nano Letters* 5, 667–673.
- Kong, J., Chapline, M.G., Dai, H.J., 2001. *Advanced Materials* 13, 1384–1386.
- Kong, J., Franklin, N.R., Zhou, C.W., Chapline, M.G., Peng, S., Cho, K.J., Dai, H.J., 2000. *Science* 287, 622–625.
- Lee, K.B., Park, S.J., Mirkin, C.A., Smith, J.C., Mrksich, M., 2002. *Science* 295, 1702–1705.
- Li, C., Curreli, M., Lin, H., Lei, B., Ishikawa, F.N., Datar, R., Cote, R.J., Thompson, M.E., Zhou, C.W., 2005. *Journal of the American Chemical Society* 127, 12484–12485.
- Li, Z., Chen, Y., Li, X., Kamins, T.I., Nauka, K., Williams, R.S., 2004. *Nano Letters* 4, 245–247.
- Panchapakesan, B., Cesarone, G., Teker, K., Wickstrom, E., 2005. *Clinical Cancer Research* 11, 9064S–19064S.
- Popels, L.C., Cary, S.C., Hutchins, D.A., Forbes, R., Pustizzi, F., Gobler, C.J., Coyne, K.J., 2003. *Limnology and Oceanography-Methods* 1, 92–102.
- Shao, N., Wickstrom, E., Panchapakesan, B., 2008. *Nanotechnology* 19, -.
- Snow, E.S., Perkins, F.K., Robinson, J.A., 2006. *Chemical Society Reviews* 35, 790–798.
- So, H.M., Won, K., Kim, Y.H., Kim, B.K., Ryu, B.H., Na, P.S., Kim, H., Lee, J.O., 2005. *Journal of the American Chemical Society* 127, 11906–11907.
- Star, A., Gabriel, J.C.P., Bradley, K., Gruner, G., 2003. *Nano Letters* 3, 459–463.
- Star, A., Joshi, V., Skarupo, S., Thomas, D., Gabriel, J.C.P., 2006a. *Journal of Physical Chemistry B* 110, 21014–21020.
- Star, A., Tu, E., Niemann, J., Gabriel, J.C.P., Joiner, C.S., Valcke, C., 2006b. *Proceedings of the National Academy of Sciences of the United States of America* 103, 921–926.
- Stern, E., Klemic, J.F., Routenberg, D.A., Wyrembak, P.N., Turner-Evans, D.B., Hamilton, A.D., Lavan, D.A., Fahmy, T.M., Reed, M.A., 2007. *Nature* 445, 519–522.
- Tang, X.W., Bangsaruntip, S., Nakayama, N., Yenilmez, E., Chang, Y.L., Wang, Q., 2006. *Nano Letters* 6, 1632–1636.
- Williams, A.J.K., Norcross, A.J., Chandler, K.A., Bingley, P.J., 2006. *Journal of Immunological Methods* 314, 170–173.